

# ESTABLISHING THE CONNECTION BETWEEN PEANUT-SHAPED BULGES AND GALACTIC BARS

KONRAD KUIJKEN<sup>1</sup>

Harvard-Smithsonian Center for Astrophysics, 60 Garden Street, Cambridge, MA 02138.

I: kuijken@cfa.harvard.edu

AND

MICHAEL R. MERRIFIELD

Department of Physics, University of Southampton, Highfield, SO9 5NH, Britain.

I: mm@phastr.soton.ac.uk

## ABSTRACT

It has been suggested that the peanut-shaped bulges seen in some edge-on disk galaxies are due to the presence of a central bar. Although bars cannot be detected photometrically in edge-on galaxies, we show that barred potentials produce a strong kinematic signature in the form of double-peaked line-of-sight velocity distributions with a characteristic “figure-of-eight” variation with radius. We have obtained spectroscopic observations of two edge-on galaxies with peanut-shaped bulges (NGC 5746 and NGC 5965), and they reveal exactly such line-of-sight velocity distributions in both their gaseous (emission line) and their stellar (absorption line) components. These observations provide strong observational evidence that peanut-shaped bulges are a by-product of bar formation.

*Subject headings:* galaxies: spiral — galaxies: kinematics and dynamics — galaxies: structure — galaxies: individual (NGC 5746, NGC 5965)

<sup>1</sup> present address: Kapteyn Instituut, PO Box 800, 9700 AV Groningen, the Netherlands

## 1. INTRODUCTION

Around 30% of disk galaxies are observed to be barred (Sellwood & Wilkinson 1993). Normal mode analysis (e.g. Hunter 1992) and N-body simulations (e.g. Sparke & Sellwood 1987) show that a global instability in self-gravitating disks provides a natural explanation for the formation of such structures. Full three-dimensional numerical simulations also show that the formation of a bar is accompanied by a buckling instability, which means that barred systems can take on a peanut shape when viewed from the side (Combes & Sanders 1981, Combes et al. 1990, Raha et al. 1991). By comparison, at least 20% of edge-on disk galaxies have boxy or peanut-shaped bulge isophotes (Shaw 1987). These percentages are sufficiently similar for it to be very tempting to conclude that all the peanut-shaped bulges are the product of central bars.

Unfortunately, the link between these two phenomena has proved difficult to establish observationally: the boxy isophotes in a galaxy's bulge are only observable photometrically if the system is close to edge on, but the presence of a bar is only generally apparent if the galaxy is viewed in a more face-on orientation. In the case of the Milky Way, where the bulge has a slight peanut shape (Weiland et al. 1994), perspective effects provide a convincing demonstration that the Galaxy also contains a bar (Blitz & Spergel 1991), but these effects are far too small to be seen in external galaxies. The only galaxy with clear photometric evidence for both a boxy bulge and a bar is NGC 4442 (Bettoni & Galletta 1994): in this case the boxy distortions are sufficiently strong that they are still apparent at an inclination of  $72^\circ$ . More circumstantial evidence for a link is provided by NGC 1381 (de Carvalho & da Costa 1987), an edge-on S0 galaxy with a box-shaped bulge and a central plateau in its radial distribution of light which is suggestive of a central bar. Similarly, for a large sample of edge-on galaxies Dettmar & Barteldrees (1990) find an association between box- or peanut-shaped bulges and a thin central component in the light distribution, which they interpret as possible edge-on bars. Finally, some nearly edge-on systems with peanut-shaped bulge isophotes such as NGC 5746 and NGC 5965 appear to have bulges which are slightly tipped with respect to the disk plane: one possible interpretation for this effect is a bar seen not quite end-on. However, none of these data establish a strong link between boxy-bulge galaxies and barred ones.

Kinematic data have also failed to provide the definitive answer to date: the only case of an edge-on, box/peanut-bulge galaxy for which there has been convincing evidence for non-axisymmetric central dynamics is, once again, the Milky Way, where the CO and HI kinematics show the characteristics of a bar (Binney et al. 1991). In external galaxies, it has been shown that peanut-shaped bulges tend to rotate cylindrically (i.e. with azimuthal velocities which are constant with height; Jarvis 1987, 1990) whereas the rotational velocity of round bulges declines with distance from their galaxies' planes (e.g. Kormendy & Illingworth 1982). The cylindrical rotation is consistent with the predictions of N-body simulations of bars, but the evidence is still circumstantial: there also exist simple two-integral axisymmetric models for boxy bulges which exhibit cylindrical rotation much like the observations (Rowley 1988).

In this *Letter* we illustrate how the presence of a central bar produces characteristic structure in the line-of-sight velocity distribution (LOSVD) of an edge-on galaxy (§2). This signature would not occur in an axisymmetric potential, and so it provides unequivocal evi-

dence for the existence of a bar. In §3, we present spectra of two galaxies with peanut-shaped bulges which show exactly the predicted LOSVDs. We can therefore conclude that these galaxies do, indeed, contain hidden bars.

## 2. THE KINEMATIC SIGNATURE OF A BAR

The kinematics of a galaxy can be understood qualitatively from study of the closed orbits allowed by the potential. The collisional nature of interstellar gas means that these orbits are a good approximation to the motions of this component. Stellar motions are somewhat more complicated, since stars have the additional degree of freedom that they can follow orbits which oscillate about the closed orbits, and there may also be significant populations of stars on irregular, chaotic orbits (e.g., Sellwood & Wilkinson 1993). Nevertheless, in a potential with a reasonable density of non-chaotic orbits, we would expect features which show up in the distribution of closed orbits to also appear in the stellar motions, perhaps somewhat broadened by the stars’ oscillations about these orbits and diluted by their superposition on any irregular component.

Figure 1(*a*) shows the observable kinematic properties — LOSVD as a function of projected radius — for the closed orbits out to a finite radius in an axisymmetric potential. As long as the density of material is falling with radius, then projection along the line of sight at a radius  $R$  produces a high observed density of material moving at the local circular speed,  $v_{los} = v_c(R)$ , together with a tail of material moving with lower line-of-sight velocities.

The orbits in a barred galaxy have been discussed extensively in the literature: examples include the articles by Contopoulos & Papayanopoulos (1980) and Athanassoula (1993). Inside the inner Lindblad resonance (ILR) in a barred potential, the closed orbits are aligned perpendicular to the bar. Between the ILR and the corotation radius (the radius at which stars orbit the galaxy at the same speed at which the bar’s pattern rotates), the orbits are distorted with their major axes aligned along the bar. In a broad region around corotation there are no closed, non-self-intersecting orbits available, and at larger radii still the orbits are only slightly elongated and aligned perpendicular to the bar. Because gas orbits cannot intersect each other or themselves, the gas is naturally forced onto the closed non-overlapping orbits allowed by the potential. Figure 1(*b*) shows these orbits projected onto the  $\{R, v_{los}\}$  plane for a particular bar model, viewed at an angle intermediate between the bar axes. Unlike the LOSVD displayed in Figure 1(*a*), this diagram is rich in features. The transitions between the different orbit families result in gaps in the diagram; the prominent gaps which give the distribution its “figure-of-eight” appearance reflect the lack of available orbits near the corotation radius.

## 3. OBSERVATIONS OF NGC 5746 AND NGC 5965

I-band CCD images of two edge-on galaxies with peanut-shaped bulges, NGC 5746 and NGC 5965, were obtained using the FLWO 48-inch telescope. These images, presented in Figs 2(*a*) and 3(*a*), clearly show the distorted isophotes of the bulges in these systems.

In order to look for the kinematic signature of the bars which may lie hidden in these two galaxies, we obtained long slit spectra along their major axes. The data were obtained using the ISIS two-armed spectrograph on the 4.2m William Herschel Telescope on the nights of 1993 June 11–12 through a slit of width 1.25 arcseconds. Tektronix CCD detectors and 1200 line/mm gratings were used in both arms of the spectrograph, producing spectra at a resolution of  $0.41\text{\AA}/\text{pixel}$ , with 2.3 pixels FWHM. In order to reduce readout noise, the data were binned on the CCDs in the spatial direction to produce a spatial resolution of 1.05 arcseconds/pixel. The red arm of the spectrograph was used to obtain spectra centered on either the  $\text{H}\alpha$  line ( $6563\text{\AA}$ ) or the triplet of CaII lines at  $\sim 8600\text{\AA}$ . Spectra from the blue arm were centered on the Mg b feature ( $5190\text{\AA}$ ). Total exposure times on these objects were 3600s on NGC 5746 and 4800s on NGC 5965.

The spectra from both arms were initially reduced using standard IRAF longslit procedures: bias subtraction, flatfielding, two-dimensional re-binning to a logarithmic wavelength scale based on calibration from bracketing Ne-Ar lamp exposures, and co-addition of multiple observations. Significant fringing in the spectra of the calcium triplet was also flatfielded out using continuum lamp exposures obtained during the course of the night. Both arms of the ISIS spectrograph have remarkably linear spectral dispersions, and low order polynomial fits produced typical RMS residuals in the wavelength solution of  $\sim 0.015\text{\AA}$ .

### 3.1 *Emission Line Spectra*

The spectra of the [NII] line at  $6583\text{\AA}$  from the two galaxies are presented in Figs. 2(*b*) and 3(*b*). We show this line from the spectral region around  $\text{H}\alpha$  because it does not lie on top of any stellar absorption features (such as  $\text{H}\alpha$  itself), and so the stellar continuum has been effectively removed from each spectrum by simply subtracting the mean galaxy luminosity profile. It is apparent that the emission lines are split into two components forming the distorted figure-of-eight shape predicted by the barred galaxy model [c.f. Fig. 1(*b*)]. Axisymmetric gas orbits, which project as straight lines in this plane [Fig. 1(*a*)] could not combine to produce these plots.

Figures 2(*b*) and 3(*b*) also show the circular rotation speeds of these galaxies obtained from the CCD images using Merrifield’s (1991) quadrature which assumes that the galaxies are axisymmetric. This method also assumes that the galaxies have a constant mass-to-light ratio, which has been shown to be a valid assumption in the central parts of other disk galaxies (e.g. Kent 1986). In each case, the value of the mass-to-light ratio was chosen to match the observed rotational velocity at large radii. At small radii, neither emission line component matches the shape of this rotation curve (as they would in an axisymmetric galaxy), but they bracket the curve as predicted by the bar model.

The photometry in Figs. 2(*a*) and 3(*a*) also shows that the peanut-shaped distortions in NGC 5746 and NGC 5965 extend to  $\sim 35$  and  $\sim 15$  arcseconds respectively. If these distortions are due to bars, then we can associate these distances with the ends of the bars and hence, presumably, the bars’ corotation radii. These numbers fit nicely with the LOSVDs presented in Figs. 2(*b*) and 3(*b*), as the split LOSVDs extend to approximately twice the corotation radius in a barred potential [c.f. Fig. 1(*b*)].

### 3.2 Absorption Line Spectra

The reduced absorption line spectra were analyzed using the unresolved gaussian decomposition (UGD) algorithm described by Kuijken & Merrifield (1993). This method extracts the stellar LOSVD from the Doppler broadening and shift in spectral lines by modeling the velocity distribution as the sum of a set of unresolved gaussian distributions with fixed means and dispersions. The best fit LOSVD is then found by convolving this model with spectra of standard stars (obtained on the same observing run with the same spectral set-up) and varying the amplitudes of the gaussian components until the galaxy spectrum is best reproduced in a least-squares sense. For the current analysis, we coadded data along the longslit spectrum until we obtained a signal-to-noise ratio of at least 20 per wavelength pixel in each spatial bin. Each LOSVD was then modeled as the sum of 21 gaussian components with means separated by  $75 \text{ km s}^{-1}$ , and dispersions of  $50 \text{ km s}^{-1}$ .

Figures 2(*c,d*) and 3(*c,d*) show the stellar LOSVDs derived from this analysis. Deconvolution of a galaxy spectrum to extract the LOSVD is an intrinsically noise-amplifying process. We therefore expect the derived LOSVDs to be somewhat noisy, even with the high signal-to-noise ratio spectra obtained from these observations. A good measure of the reliability of the results can be obtained by comparing the LOSVDs obtained from the Mg b spectra taken with the blue arm of the spectrograph with those obtained from absorption line spectra taken with its red arm. In the case of NGC 5746, these red arm spectra were centered on the calcium triplet; for NGC 5965, the spectra used were all centered on the H $\alpha$  line (with the emission lines automatically rejected from the UGD fitting process [Kuijken & Merrifield 1993]). The two arms of the spectrograph are essentially independent instruments which obtain spectra with different CCD responses, different velocity resolutions, different contamination from night sky lines, etc. There are therefore not likely to be any strong common systematic problems, and so differences between the derived LOSVDs can be attributed to the uncertainty due to the finite signal-to-noise ratio of the data. By comparing parts (*c*) and (*d*) of Figs. 2 and 3, it is apparent that even quite subtle structure in the LOSVDs is reproduced in these independent data sets. In particular, the clear split into two components, one faster than the circular speed and one slower than the circular speed, mirrors the behavior of the emission line spectra.

The similarity between the LOSVDs derived from different parts of the spectrum also allows us to address any concerns about the effects of extinction in these galaxies. Inspection of the photometry in Figs. 2(*a*) and 3(*a*) reveals that, although these disk galaxies are of early Hubble types, they do show some obscuration by dust lanes. The galaxies' inclinations mean that the lines of sight of our spectral observations will intersect the dust lanes midway through each galaxy. The observed structure in the LOSVDs might therefore be the result of selective dust extinction along these lines of sight through intrinsically axisymmetric galaxies. However, the close agreement between the LOSVDs derived from the red and blue spectral data belies this explanation. In the case of NGC 5746, for example, the sizes of the high velocity components (which would come from material at the smallest radii in an axisymmetric galaxy) are identical to within the observational errors of  $\sim 30\%$ . From the standard interstellar extinction curve (e.g. Mihalas & Binney 1981), the difference between the extinction at  $5200\text{\AA}$  and that at  $8600\text{\AA}$  can only be less than 30% if the extinction at  $8600\text{\AA}$  is less than 0.4 magnitudes. No matter how such a modest amount of extinction is

distributed along the line of sight, it is nowhere near enough to explain the gap between the slow and fast components in the LOSVD, where the projected phase density is depressed by at least a factor of 5.

#### 4. DISCUSSION

An edge-on barred galaxy displays a characteristic kinematic signature in that its LOSVD has two high density peaks. One of these peaks travels faster than the local circular speed, the other more slowly, and the variation in their velocities with projected radius along the major axis forms a distorted figure-of-eight in the  $\{R, v_{los}\}$  plane. This signature allows edge-on barred galaxies to be identified. We have used this indicator in optical spectra to show that the two galaxies with peanut-shaped bulges which we have studied — NGC 5746 and NGC 5965 — also harbor bars. This discovery provides strong observational support for the hypothesis that peanut-shaped and boxy bulges are a by-product of bar formation.

Binney et al. (1991) have demonstrated that CO and HI observations reveal the presence of a bar at the center of the Milky Way. We might therefore expect that data in these wavebands from external galaxies should also show the sort of signature that we have found in optical observations. Indeed, CO observations of the edge-on boxy-bulged S0 galaxy NGC 4710 (Wrobel & Kenney 1992) show exactly the same two-component velocity distribution, and we would suggest this observation implies that NGC 4710 also contains a bar.

With the current generation of 4-meter telescopes and efficient spectrographs, it is possible to obtain spectra of the central parts of external galaxies at high signal-to-noise ratios. As we have shown, such spectra are of sufficient quality to study quite fine kinematic structure in both the gaseous and stellar components of these systems. Further comparison of kinematic data from peanut-shaped bulges with detailed dynamical models of bars will enable us to explore the connection between these two phenomena in much greater depth.

KK was supported by a Hubble Fellowship through grant HF-1020.01-91A awarded by the Space Telescope Science Institute (which is operated by the Association of Universities for Research in Astronomy, Inc., for NASA under contract NAS5-26555). MM was supported by a PPARC Advanced Fellowship (B/94/AF/1840). The spectral observations were obtained with the William Herschel Telescope, operated on the island of La Palma by the Royal Greenwich Observatory in the Spanish Observatorio del Roque de los Muchachos of the Instituto de Astrofísica de Canarias. We thank Reynier Peletier for his assistance with the observations, and Marijn Franx for a thorough reading of the manuscript.

#### REFERENCES

- Athanassoula, E., MNRAS, 259, 328
- Bettoni, D. & Galletta, G. 1994, A&A, 281, 1
- Binney, J., Gerhard, O.E., Stark, A.A., Bally, J. & Uchida, K.I. 1991, MNRAS, 252, 210
- Binney, J. & Tremaine, S. 1987, Galactic Dynamics (Princeton: Princeton University Press)

Blitz, L. & Spergel, D.N. 1991, ApJ, 379, 631  
Combes, F., Debbasch, F., Friedli, D. & Pfenniger, D. 1990, A&A, 233, 82  
Combes, F. & Sanders, R.H. 1981, A&A, 96, 164  
Contopoulos, G. & Papayannopoulos, Th.D., 1980, A&A, 92, 33  
de Carvalho, R.R. & da Costa, L.N. 1987, A&A, 171, 66  
Dettmar, R.-J. & Barteldrees, A. 1990, in ESO/CTIO workshop on bulges of galaxies, 259.  
Hunter, C. 1992, in Astrophysical Disks, eds S.F. Dermott, J.H. Hunter & R.E. Wilson (New York: New York Academy of Sciences), 22  
Jarvis, B.J. 1987, AJ, 94, 30  
Jarvis, B.J. 1990, in Heidelberg Conference on the Dynamics and interactions of galaxies, ed. R. Wielen (Springer), 416  
Kent, S.M. 1986, AJ, 91, 1301  
Kormendy, J. & Illingworth, G. 1982, ApJ, 256, 460  
Kuijken, K. & Merrifield, M.R. 1993, MNRAS, 264, 712  
Merrifield, M.R. 1991, AJ, 102, 1335  
Mihalas, D. & Binney, J. 1981, Galactic Astronomy (New York: Freeman)  
Mulder, W.A. & Liem, B.T. 1986, A&A, 157, 148  
Raha, N., Sellwood, J.A., James, R.A. & Kahn, F.D. 1991, Nature, 352, 411  
Rowley, G. 1988, ApJ, 331, 124  
Sellwood, J.A. & Wilkinson, A. 1993, Rep Prog Phys, 56, 173  
Shaw, M.A. 1987, MNRAS, 229, 691  
Sparke, L.S. & Sellwood, J.A. 1987, MNRAS, 225, 653  
Weiland, J.L. et al. 1994, ApJ, 425, L81  
Wrobel & Kenney 1992, ApJ, 399, 94

## FIGURE CAPTIONS

FIG. 1—Orbits projected into the observable  $\{R, v_{los}\}$  plane for an edge-on galaxy with potential  $\Psi(R, \theta) = 0.5 \ln(0.2^2 + r^2) - [1 + r^2(1 + \epsilon \cos 2\theta)]^{-1.5}$  at an intermediate position angle. Orbits are randomly sampled, and plotted with symbols of sizes which mimic a radial exponential density law of unit scale length. (a) axisymmetric potential,  $\epsilon = 0$ , and (b) barred potential,  $\epsilon = 0.2$ . The pattern speed is such that the corotation radius of the barred potential occurs at a radius of unity.

FIG. 2—Photometry and kinematics of NGC 5746. (a) I-band photometry of the galaxy, with contours spaced by 0.3 magnitudes: the thick line indicates the position of the slit for the spectral observations. Line-of-sight velocity distribution, normalized to unit velocity integral, as a function of projected radius for: (b) the gaseous component as traced by the [NII] line at 6583Å; (c) the stellar component as derived from absorption lines around the Mg b feature at 5170Å; and (d) the stellar component as derived from absorption lines around the Ca triplet at 8600Å. The greyscale bar indicates the relative phase space density scale in both (c) and (d).

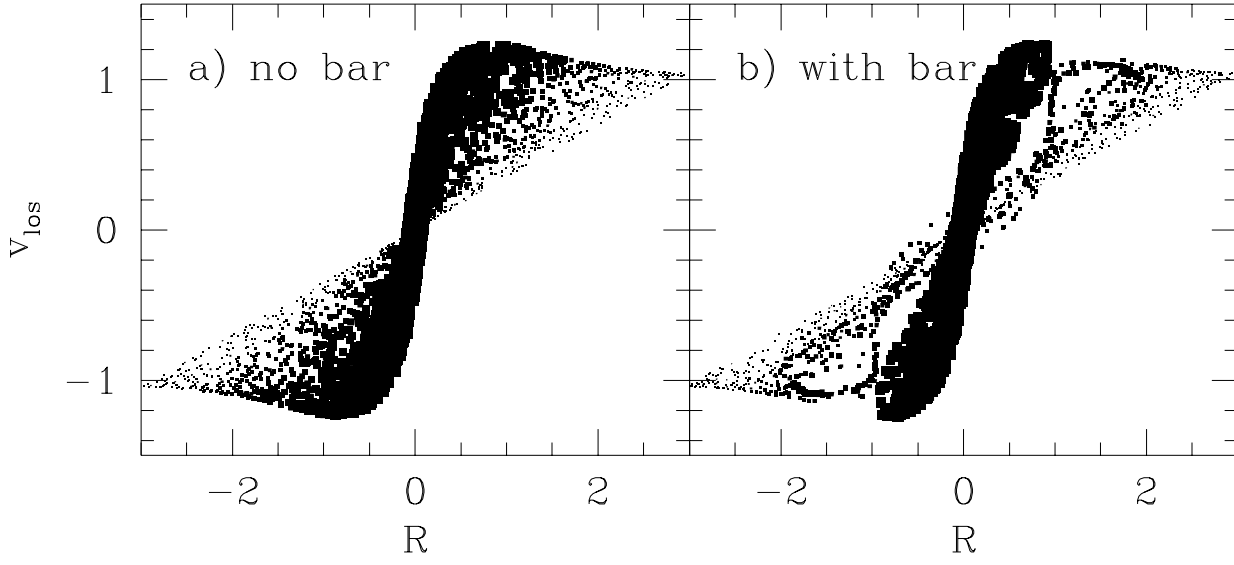
FIG. 3—Photometry and kinematics of NGC 5965. (a) I-band photometry of the galaxy, with contours spaced by 0.3 magnitudes: the thick line indicates the position of the slit for the spectral observations; the diagonal feature is due to a bad column in the CCD. Line-of-sight velocity distribution, normalized to unit velocity integral, as a function of projected radius for: (b) the gaseous component as traced by the [NII] line at 6583Å; (c) the stellar component as derived from absorption lines around the Mg b feature at 5170Å; and (d) the stellar component as derived from absorption lines around the H $\alpha$  line at 6563Å. The greyscale bar indicates the relative phase space density scale in both (c) and (d). The absence of strong absorption features and contamination by emission lines limit the signal-to-noise ratio in (d).



This figure "fig1-1.png" is available in "png" format from:

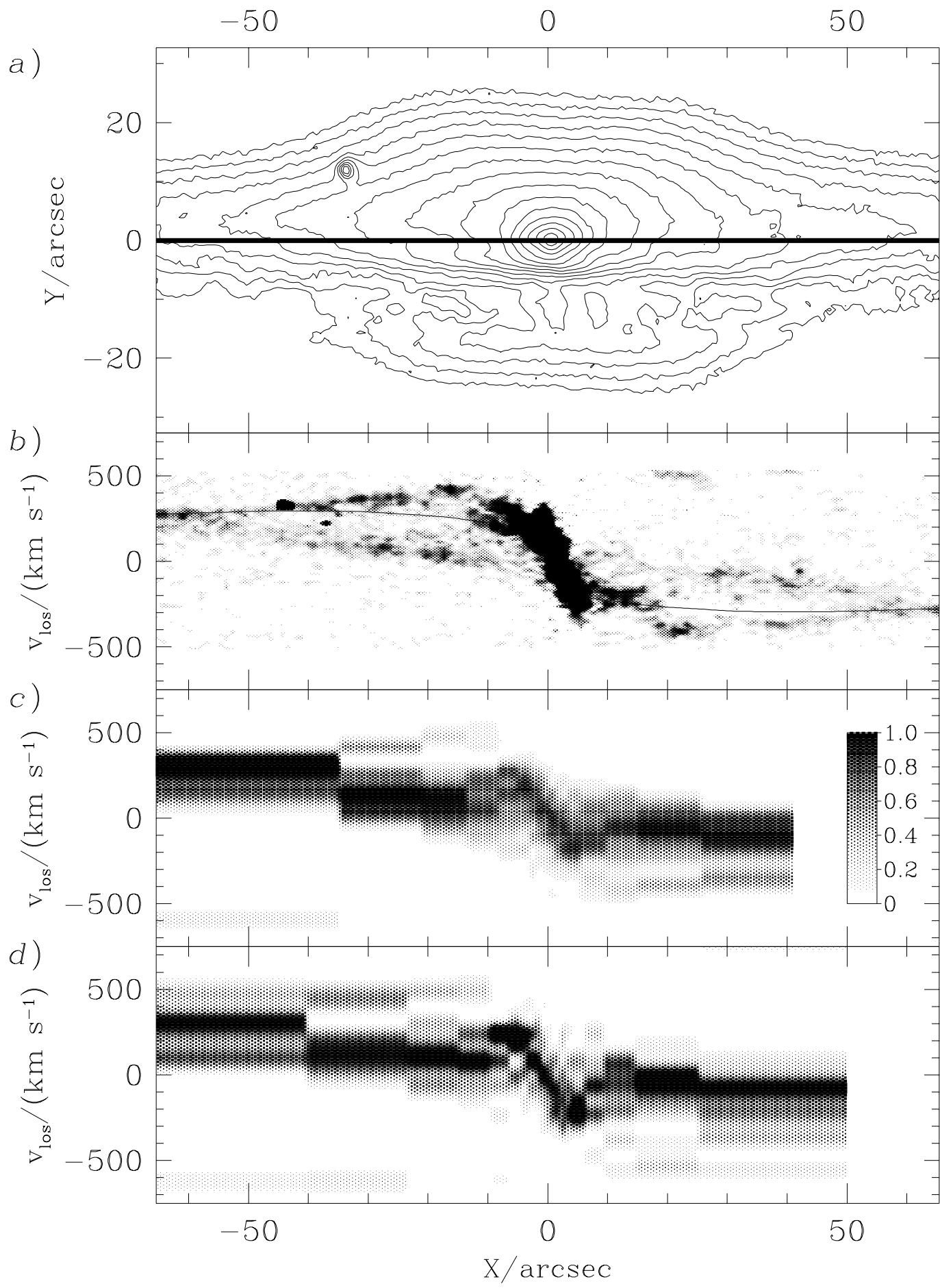
<http://arxiv.org/ps/astro-ph/9501114v1>

*l-v diagrams to l=45*



This figure "fig1-2.png" is available in "png" format from:

<http://arxiv.org/ps/astro-ph/9501114v1>



This figure "fig1-3.png" is available in "png" format from:

<http://arxiv.org/ps/astro-ph/9501114v1>

